Sonderforschungsbereich/Transregio 40
Proceedings of the Summer Program 2013

Large Eddy Simulation of a Subscale Combustion Chamber

By T. Dawson[†], S. Menon[†] AND O. J. Haidn[‡]

[†]School of Aerospace Engineering, Georgia Institute of Technology Atlanta, GA, USA
[‡] Fachgebiet Raumfahrtantriebe, Lehrstuhl für Flugantriebe, Technische Universität München

Oxy-methane combustion is becoming an increasingly viable option for rocket systems, but the current body of knowledge regarding its use in such applications is lacking in key areas such as injector design, jet interactions, and bulk heat transfer characteristics. For this reason, an experimental facility has been constructed at Technische Universität München (TUM) with the intent of conducting research on subscale subcritical rocket combustion chambers, beginning with a single coaxial injector configuration using gaseous oxygen and methane. In this report, Large Eddy Simulation (LES) of this single injector configuration is performed on a relatively coarse grid to evaluate its ability to characterize the flame structure. The flame structure and its anchoring, the LES quality and the flowfield are all examined and some preliminary comparison with the experimentally measured wall pressure data is carried out.

1. Introduction

Although LOX/methane is an attractive option for rocket engines there is limited knowledge and data for oxy-methane combustion at the extreme conditions representative of a rocket. Of particular interest are injector technology and heat transfer characteristics; to this end, experimental facilities were recently developed in the Institute for Flight Propulsion (LFA) at Technische Universität München (TUM) to document detailed wall heat flux characteristics in representative subscale combustion chambers with single and multi-injector configurations. At this time the focus is on shear co-axial injection of gaseous oxygen and methane (GOX-GCH4) over a range of pressure from 5 to 40 depending on the configuration.

A single injector configuration is fully operational and experimental data is available at pressures up to 20 bar and varied equivalence ratios. This data includes wall pressures and temperatures at multiple locations along the axial direction. In the context of the summer research program SFB/TRR 40, an initial attempt is made here to simulate this experiment using Large Eddy Simulation (LES). For this exploratory look, a relatively coarse grid and a reduced two-step oxy-methane chemistry mechanism without subgrid closure of turbulence-chemistry interactions are used along with adiabatic wall conditions. Thus, there are some drastic simplifications and differences from the experiment, but the focus is to determine if LES can provide a qualitative first look at the flame structure and flow features. We report below on the observations from this study.

Injector		
GOX diameter	(mm)	4
GOX post wall thickness	(mm)	0.5
GCH4 diameter	(mm)	6
GOX post length	(mm)	96
GCH4 post length	(mm)	44

Chamber		
Chamber length	(mm)	290
Cross sectional area	(mm^2)	12x12
Throat area	(mm^2)	12x4.8

TABLE 1. Combustion Chamber Dimensions.

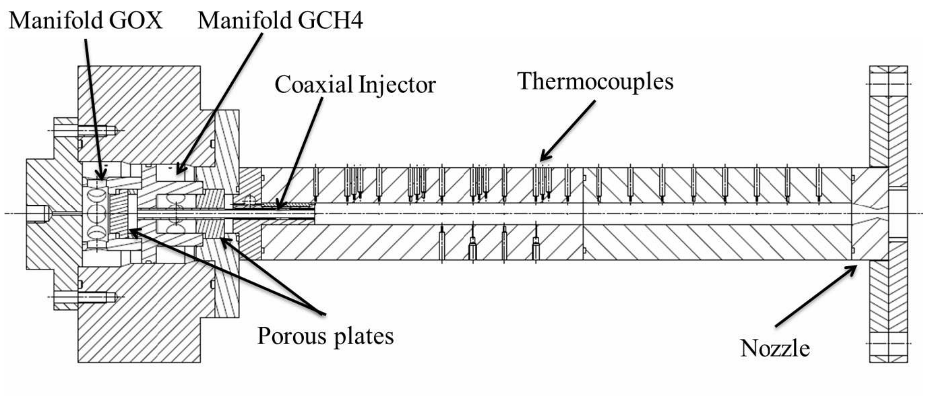

FIGURE 1. Experimental Test Facility at TUM.

2. Experiment Overview

The combustion chamber, as shown in Figure 1, consists of a square cross section truncated with a supersonic nozzle. The relevant dimensions are summarized in Tab. 1, with the chamber length measured from the faceplate to the nozzle throat. The oxidizer tube is flush with the injection plane. The oxidizer and fuel are fed into individual manifolds via a constant mass flow choked orifices, and uniform injection temperatures and pressures are ensured using porous plates with measured pressure and temperature drop across them.

The chamber walls contain 9 pressure transducers (not shown) and 29 thermocouples positioned axially along the chamber centerline as depicted. The pressure readings are configured to measure the static pressure distribution at the wall at 34 mm intervals, and collect data up to 100 Hz. Meanwhile, the thermocouples are located at varying depths into the wall at 17 mm intervals in order to measure heat transfer properties; 17 are located at a depth of 1 mm, while four each are flush mounted, and at 2 and 3 mm into the wall.

		Experiment	Simulation
OF Ratio	-	3.48	3.48
Chamber Pressure	(bar)	19.2	19.6
GOx Pressure*	(bar)	27.5	21.3
GCH4 Pressure*	(bar)	23	21.4
GOX Mass Flow	(g/s)	49.1	49.1
GCH4 Mass Flow	(g/s)	14.1	14.1
GOX Velocity	(m/s)	-	143
GCH4 Velocity	(m/s)	-	118
GOX Temperature	(K)	281.7	281.7
GCH4 Temperature	(K)	280.5	280.5

TABLE 2. Operating Conditions.

OF Ratio	-	3.43
GOX Bulk Velocity	(m/s)	169
GCH4 Bulk Velocity	(m/s)	150
Density Ratio, S	-	0.51
Velocity Ratio, R	-	0.89
Mass Flux Ratio, J	-	0.40
$Re^*_{Coaxial}$	-	$1 \cdot 10^6$

TABLE 3. Injection Characteristics.

The chamber operates in a pressure range from 5 to 20 bar, with oxidizer-fuel (OF) mass ratios from 2.6 to 3.4. A single case is selected for the LES study, and Tab. 2 lists both the design point and the operating conditions of the simulation. The reactant pressure and temperatures are as measured in their respective manifolds in the experiment, and at the inlet plane in the simulations.

The flow is characterized by the non-dimensional parameters listed in Tab. 3, where the bulk velocity is the average velocity measured at the exit plane of the injector in the simulations, and the mass flux ratio J is defined as the reactant density ratio, S, multiplied by the velocity ratio squared, $S\,R^2 = J$. The Reynolds number for a coaxial jet such as this is then estimated as [1]:

$$Re^* = \left(\frac{\rho_F d_F V_F}{\mu_F}\right)\left[1 + \frac{1-J}{J}\left(\frac{d_{Ox}}{d_F}\right)^2\right]^{1/2} \tag{2.1}$$

Here, the subscripts Ox and F refer to oxidizer and fuel respectively, and d_{Ox} and d_F are the respective diameter. The Reynolds number clearly indicates that a highly turbulent shear layer is to be expected, and proper resolution of this is required.

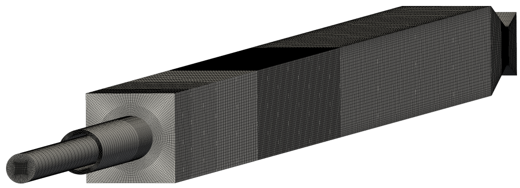

(a) Original coarse grid.

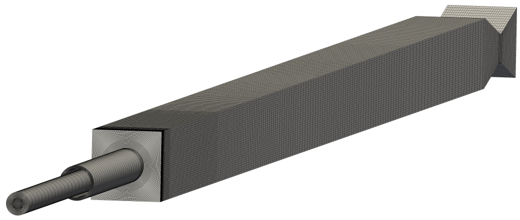

(b) Current grid.

FIGURE 2. Computational domain.

3. Numerical Method, Setup and Assessment

The current numerical solver solves the Favre-filtered compressible, multi-species Navier-Stokes equations, which are not shown here for brevity. The subgrid momentum and energy fluxes are modeled using an eddy viscosity closure for which a transport equation for the subgrid kinetic energy is solved along with the LES equations. The filtered reaction rates are obtained in terms of the resolved flow variables and thus, subgrid turbulence-chemistry interactions are neglected at this time.

The numerical solver is a well established finite-volume, block-structured parallel solver called LESLIE that has been used for such studies [2–4]. The solver employs a hybrid method that combines a 3^{rd} order upwind numerical scheme with MUSCL reconstruction alongside an approximate Riemann solver and a 2^{nd} order central scheme for spatial integration. Temporal accuracy is 2^{nd} order. The hybrid method automatically uses local sensors based on pressure and density gradients to switch from the central scheme to the upwind scheme in regions of high gradients [3,4]. A two-step, five species (CH_4, O_2, CO_2, CO, and H_2O) reduced chemistry mechanism is used for the finite-rate chemistry, adapted from the 2S_CH4BFER mechanism by Franzelli et al. [5] for use with oxy-methane. This mechanism has been used recently on similar high-pressure oxy-methane combustion simulations [6] with reasonable accuracy in prediction. The mechanism is employed with a thermally perfect equation of state and power-law transport models.

The inflow boundary conditions use constant mass Navier Stokes Characteristic Boundary Conditions (NSCBC) [7] to mimic the constant mass flow conditions at the experimental inlet, while the outflow is supersonic. The walls are no-slip and adiabatic, and while the neglected heat flux is expected to cause an increase of the mean chamber pressure, it is expected to provide a reasonable approximation of the flame structure. More accurate treatment of the wall conditions are planned for a future study.

The computational domain has undergone two major iterations due to multiple problems with the grid quality and its setup. The original grid's employed both a coarse spacing near the injector (nearly 0.3 mm in the axial direction) and also used two grid coarsenings in the axial direction, across which the solution was interpolated onto a coarser mesh to reduce the overall computational cost. The computed flow field showed

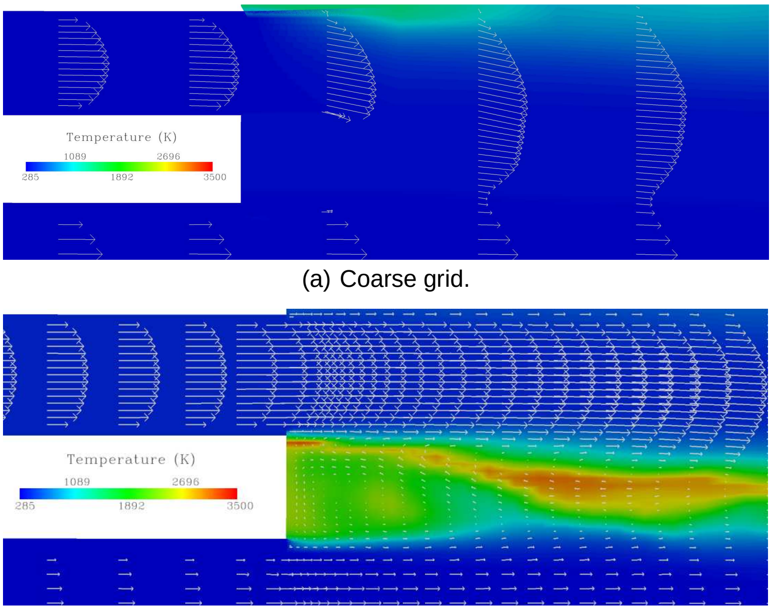

(a) Coarse grid.

(b) Current grid.

FIGURE 3. Oxidizer post tip temperature field overlaid with velocity vectors.

a lifted flame since the region near the flame anchoring point was poorly resolved. A more refined grid with the spacing down to 30 $\mu\mathrm{m}$ in both axial and radial directions in the shear layer region is now used and without any grid coarsening to eliminate any possibility of grid related issues. For comparison, the original and final grids are shown in Fig. 2. The grids are multi-block structured Cartesian grids, and the final grid contains 3.6 million points, which is nearly double of the original one. More details are provided below but it is emphasized that grid independence studies will be addressed in the near future.

To highlight the most obvious physical manifestation of the original coarse grid's inability to obtain an anchored flame, we show the flow and the flame structure near the injector post-tip region. As shown in Fig. 3, which overlays an instantaneous temperature field from the respective simulation with velocity vectors, in the original coarse grid case Fig. 3(a), there is no flame anchored at the tip, and there is also no reverse flow in the base of the post-tip, whereas the current grid result shown in Fig. 3(b) is able to capture the vortices and hold the flame.

Refining the grid was not sufficient to prevent the flame from lifting off, and further analysis revealed that the grid coarsening plane was generating spurious waves in the velocity field, as shown in Fig. 4. This feature of the LESLIE code has been used previously with great success, but was not implemented correctly here. While this issue remains to be resolved, we remove all grid coarsening features for the reported simulations.

The shear layer is now resolved with 17 grid points with spacing of 30 $\mu\mathrm{m}$. This grid spacing appears reasonable for resolution of the shear-layer turbulence using the current LES by examining the resolved kinetic energy spectra in the shear layer at a location 1.7 injector diameters downstream (x=10 mm), shown here in Fig. 5. The spectrum

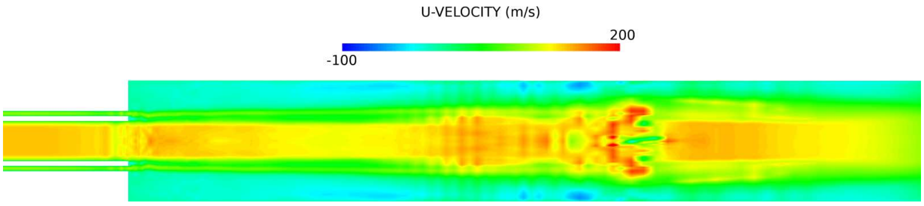

FIGURE 4. Spurious waves in the axial velocity field when an incorrect grid coarsening is used.

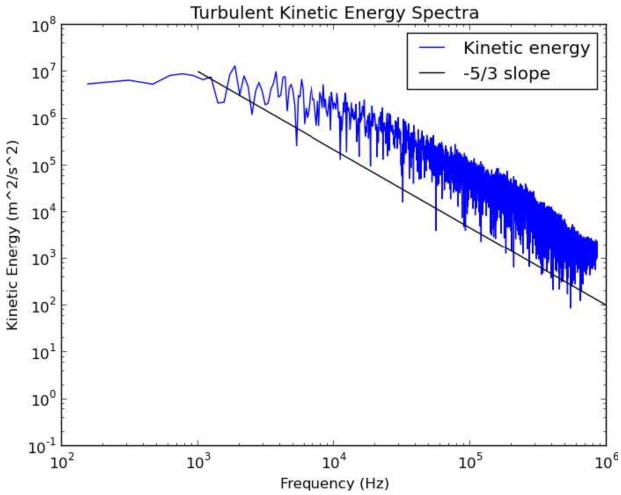

FIGURE 5. Kinetic energy spectrum at x = 10 mm in the shear layer.

demonstrates that the turbulence energy cascade maintains the proper Kolmogorov -5/3 slope in the resolved inertial range [8] at least in this region.

To quantify the resolution of turbulence in the near-injector shear layer the subgrid turbulent kinetic energy, k_{sgs}, is shown in Fig. 6(a). A more quantifiable measure of the LES quality is the Pope Criteria, which is defined as the ratio of the sub-grid kinetic energy to the total kinetic energy:

$$M_{res} = \frac{\langle k_{sgs} \rangle_T}{\langle k_{sgs} \rangle_T + k_{res}} \tag{3.1}$$

where k_{res} is the resolved turbulent kinetic energy, defined as the mean squared velocity fluctuations, $1/2 \langle \sum (\tilde{u}_i - \langle \tilde{u}_i \rangle_T)^2 \rangle_T$, and $\langle \cdot \rangle_T$ is the time-averaging operator. It has been argued that for LES $M_{res} \leq 0.2$ is needed and although the exact number is debatable, it can been seen in Fig. 6(b) by overlaying the Pope Criteria field that there is still insufficient resolution in the inlet pipe boundary layers and near-injector field region. This is very likely due to the wall grid employed and the lack of wall models causing an over prediction of k_{sgs}. This issue is known and future studies will incorporate wall modeling for both the near-wall turbulence and heat transfer.

4. Results and Discussion

The primary goal of this investigation is to obtain a qualitative look at the flame structure and flow-flame interactions using LES. Future studies are planned to address some

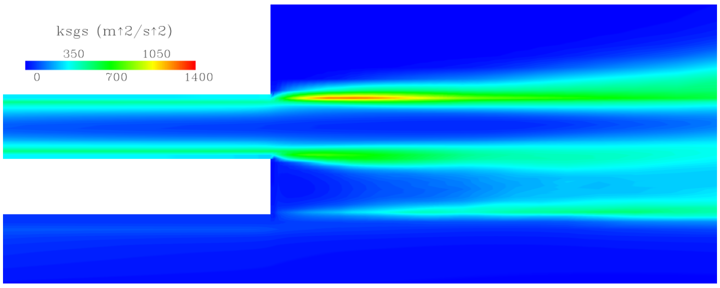

(a) Subgrid Kinetic Energy.

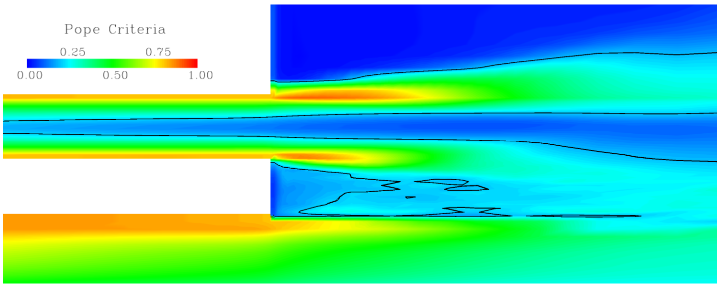

(b) Pope Criteria, $M_{res} = 20\%$ isoline in black.

FIGURE 6. LES quality assessment in the near-injector shear region.

of the limitations in the current effort including grid resolution, turbulence-chemistry closure and isothermal wall. In the following sections, the temperature, axial velocity, and reactant species are examined in an instantaneous and a time-averaged sense to qualitatively show the lifted flame structure. The time-averaged fields have been obtained by averaging over 8 flow through times of the instantaneous flow field. Using the Intel PC cluster in the Computational Combustion Laboratory at Georgia Tech, a typical flow through time takes around 12 wall clock hours using 1248 cores.

We compare the instantaneous (top half) and time-averaged (bottom half) views of the flow fields in the following figures. The flame appears to be very long, approximately 90 mm as outlined by the T=2200 K isoline in Fig. 7(a). The CH_4 mass fraction, shown in Fig. 7(c), shows that most of the fuel remains close to the walls and a large portion appears in the recirculation behind the dump wall, transported by a large corner recirculation zone of which the mean boundary is outlined in the time-averaged velocity figure in Fig. 7(b) with a black line. The mean CH_4 mass fraction in the center of the recirculation quickly plateaus at a mean value of 0.8 although further studies are needed to determine how much of the fuel remains trapped in the recirculation. Meanwhile, Fig. 7(d) shows a significant portion of O_2 remains unconsumed downstream for this test case.

The recirculation zone and the asymmetric nature of the instantaneous flow field is better visualized using spanwise slices of the chamber. The reverse flow is strongest at the wall corners, as shown by the axial velocity magnitude in Fig. 8(a), where the blue region represents flow towards the injection plane. Interestingly, the recirculation zone is not especially hot, and the cool oxygen core is still intact at 80 mm downstream (Fig. 8(b)). Instantaneously, local pockets show temperature peaking up to 4200 K, which is an over-prediction from the adiabatic value. This is a consequence of the coarse grid and reduced kinetics employed here as well as the lack of subgrid turbulence-chemistry closure, and all will be addressed in future studies.

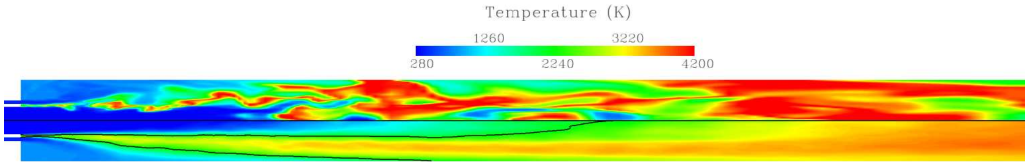

(a) Temperature with T=2200 K isoline.

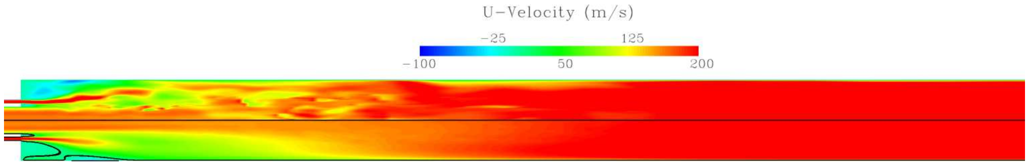

(b) Axial Velocity with u=0 m/s isoline.

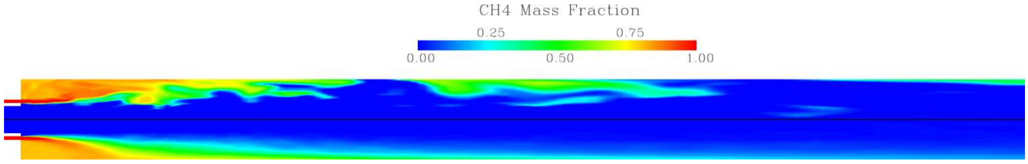

(c) CH_4 Mass Fraction.

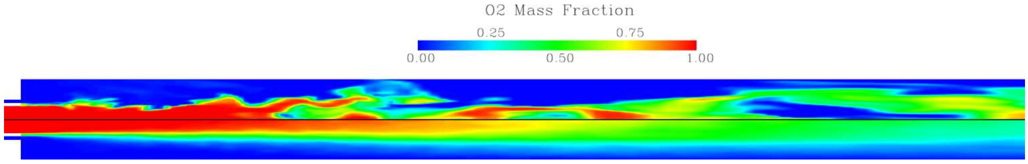

(d) O_2 Mass Fraction.

FIGURE 7. Instantaneous (top half) and mean (bottom half) iso-contours of flow variables.

Since this is a non-premixed flame, it should burn as a diffusion flame anchored at the post tip. To facilitate understanding of the flame anchoring, we utilize the indexed fuel reaction rate ($\dot{\omega}_F^*$) based on the Takeno flame index (FI), as defined earlier in [9]. The reaction rate tracks the flame surface and the flame index indicates the local burning mode, i.e., whether it is a premixed or diffusion flame. The indexed reaction rate retains both properties, and is defined as:

$$\dot{\omega}_F^* = \frac{\nabla Y_{CH_4} \cdot \nabla Y_{O_2}}{|\nabla Y_{CH_4} \cdot \nabla Y_{O_2}|} |\dot{\omega}_{CH_4}| \tag{4.1}$$

A positive value of flame index (and therefore $\dot{\omega}_F^*$) indicates that the flame is locally premixed, while a negative value indicates a diffusion flame. Figure 9 shows the indexed reaction rate plotted along axial and transverse slices, and as expected the flame is primarily a diffusion flame. However, small pockets of premixed (and/or partially premixed) combustion appear in the outer regions of the shear layer with more pockets seen closer to the combustor wall and recirculation regions. Although partially premixed and premixed combustion have been seen in other shear-coaxial injector systems [6] further studies are still required here before making any firm conclusions.

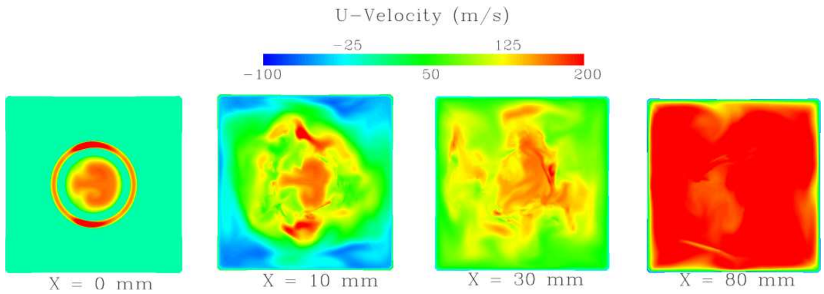

(a) Axial Velocity.

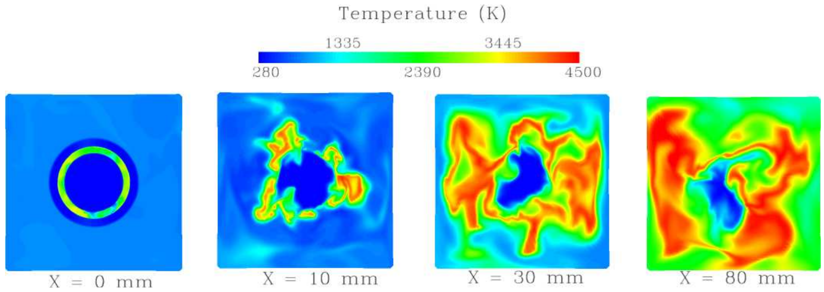

(b) Temperature.

FIGURE 8. Instantaneous spanwise axial velocity and temperature iso-contours.

An assessment of the predicted pressure is carried out by comparing with the experimentally measured data even though wall conditions are not the same. The wall pressures are normalized by the mean chamber pressure, as $(p-\overline{p})/\overline{p}$, and compared in Fig. 10. The overall trend is captured, with the peak occurring near the same axial location but with an increase in magnitude of nearly 1% in the simulation. Additionally, the mean pressure was approximately 2% higher in the simulation, measured as 19.6 bar as compared to 19.2 bar in the experiment. These discrepancies need to be explained and will be the focus of future studies.

5. Conclusions and Future Plans

Large Eddy Simulation is applied to an experimental oxy-methane combustion rig using relatively coarse grids and a 2-step reduced chemistry mechanism without any subgrid turbulence-chemistry interaction closure. The importance of the grid quality is revealed from these studies and its impact on flame holding is assessed. Too coarse of a grid and the flame can be lifted (numerically), whereas, with a reasonably refined grid, a diffusion flame is anchored (on or near) the injector post tip. Although the latter result is more realistic, further grid resolution studies are still needed and planned. Future studies will also focus on comparison with the heat transfer data, which will require isothermal wall conditions, and on applying a subgrid turbulence-chemistry interaction closure [2, 6] for this test case. Collaboration with the experimental group in TUM will be continued in this effort.

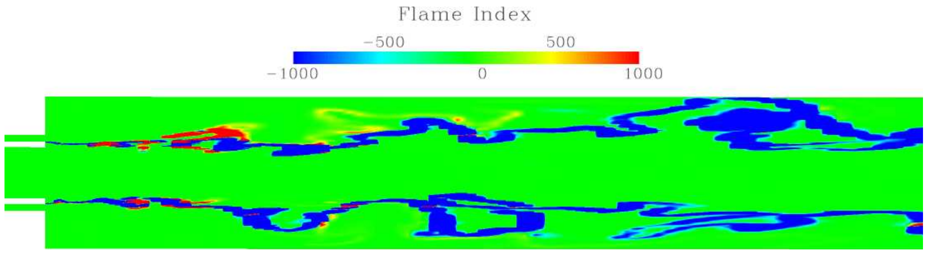

(a) Axial.

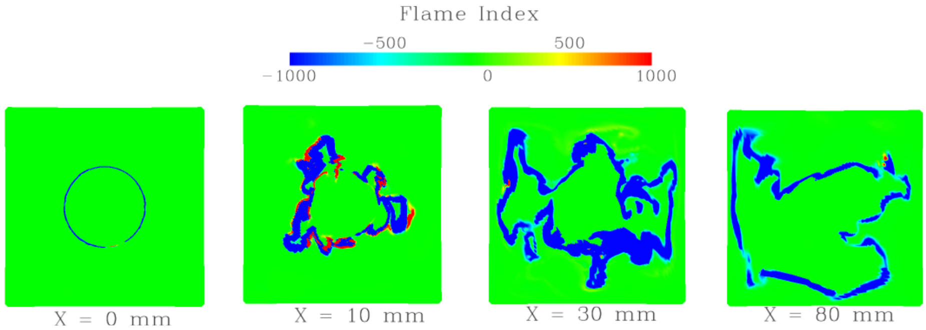

(b) Spanwise.

FIGURE 9. Instantaneous indexed reaction rate in the axial and spanwise views.

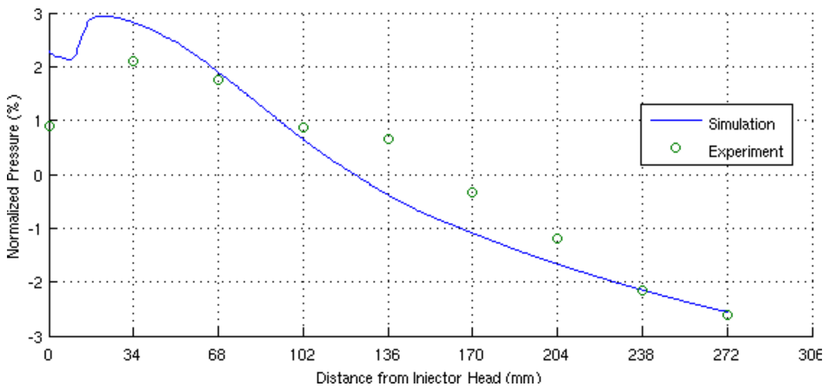

FIGURE 10. Wall pressure comparison.

Acknowledgments

Financial support is provided by the German Research Foundation (Deutsche Forschungsgemeinschaft – DFG) in the framework of the Sonderforschungsbereich/Transregio 40 and the International Graduate School of Science and Engineering (IGSSE) at Technische Universität München. Additional support for TD is provided by US Air Force Office of Scientific Research (Dr. Mitat Birkan, Program Manager). Computations were carried out at the Georgia Tech Cluster and at the US Department of Defense HPC centers. We also acknowledge support and guidance by Prof. Oskar Haidn and his research group for providing their data and help in setting up the simulations.

References

[1] SCHUMAKER, S. A. AND DRISCOLL, J. F. (2012). Mixing properties of coaxial jets with large velocity ratios and large inverse density ratios. *Physics of Fluids*, **24**, 055101-1–21.

[2] MENON, S. AND PATEL, N. (2006). Subgrid modeling for simulation of spray combustion in large-scale combustors. *AIAA Journal*, **44**, 709–723.

[3] MASQUELET, M. AND MENON, S. (2010). Large eddy simulation of flame-turbulence interactions in a shear coaxial injector. *Journal of Propulsion and Power*, **26**, 924–935.

[4] GENIN, F. AND MENON, S. (2010). Studies of shock/turbulent shear layer interaction using large-eddy simulation. *Computers and Fluids*, **39**, 800–819.

[5] FRANZELLI, B., RIBER, E., GIQUEL, L. Y. M. AND POINSOT, T. (2010). Large-Eddy Simulation of combustion instabilities in a lean partially premixed swirled flame. *Combustion and Flame*, **159**(2), 621–637.

[6] GUÉZENNEC, N., DAWSON, T., SIERRA, P. AND MENON, S. (2013). Flame holding dynamics during combustion instability in a shear-coaxial injector combustor. *International Symposium on Turbulence and Shear Flow Phenomena 8*.

[7] POINSOT, T. J. AND LELE, S. K. (1992). Boundary conditions for direct simulations of compressible viscous flows. *Journal of Computational Physics*, **101**, 104–129.

[8] POPE, S. B. (2000). *Turbulent Flows*. Cambridge University Press.

[9] PATEL, N. AND MENON, S. (2008). Simulation of spray turbulence flame interactions in a lean direct injection combustor. *Combustion and Flame*, **153**, 228–257.